Selective and ATP-dependent Translocation of Peptides by the Homodimeric ATP Binding Cassette Transporter TAP-like (ABCB9)*

Justina Clarinda Wolters, Rupert Abele‡, and Robert Tampé§

From the Institute of Biochemistry, Biocenter, Johann Wolfgang Goethe-University Frankfurt, Marie-Curie-Str. 9, D-60439 Frankfurt/M., Germany

The transporter associated with antigen processing (TAP)-like (TAPL, ABCB9) belongs to the ATP-binding cassette transporter family, which translocates a vast variety of solutes across membranes. The function of this half-size transporter has not yet been determined. Here, we show that TAPL forms a homodimeric complex, which translocates peptides across the membrane. Peptide transport strictly requires ATP hydrolysis. The transport follows Michaelis-Menten kinetics with low affinity and high capacity. Different nucleotides bind and energize the transport with a slight predilection for purine bases. The peptide specificity is very broad, ranging from 6-mer up to at least 59-mer peptides with a preference for 23-mers. Peptides are recognized via their backbone, including the free N and C termini as well as side chain interactions. Although related to TAP, TAPL is unique as far as its interaction partners, transport properties, and substrate specificities are concerned, thus excluding that TAPL is part of the peptide-loading complex in the classic route of antigen processing via major histocompatibility complex class I molecules.

ATP-binding cassette (ABC)[1] transporters resemble one of the largest family of membrane proteins. They translocate a broad spectrum of solutes across membranes by converting the chemical energy of ATP into mechanic movement (1, 2). In special cases, they can operate as ion channels or regulators. 49 ABC transporters have been identified in the human, which can be divided into seven subfamilies (A–F) (3). The subfamily B with 11 members comprises the multidrug resistance proteins (MDR1, MDR3) and the transporter associated with antigen processing (TAP1 and TAP2). This heterogeneous subfamily includes full-size and half-size transporters, the latter must assemble to homodimers or heterodimers. The next degree of intricacy is that members of this subfamily are found in different subcellular compartments, such as the plasma membrane, the endoplasmic reticulum, the lysosome, or the inner mitochondrial membrane. Function and substrate specificity could be determined for only five members (MDR1, MDR3, TAP1/2, and BSEP) but not for the others, especially not for ABCB9.

ABCB9 shares 38% sequence identity to TAP1 and 40% to TAP2, which is also mirrored by the genomic organization (4, 5). All three half-size transporters consist of 11 coding exons, whereas TAP2 and TAPL contain an additional non-coding exon upstream of the translation start (6). Moreover, the exon length is almost identical in TAP and TAPL. In addition, C-terminal splice variants of TAPL, similar to TAP2, have been identified (6, 7). Based on this sequence homology, ABCB9 is called TAP-like (TAPL) and categorized together with TAP1 and TAP2 into the TAP family, although nothing is known about the TAPL function.

Based on mRNA level, TAPL is highly expressed in testes, moderately in the brain and spinal cord, and at low level in other tissues (4, 5). Conflicting data exist regarding the subcellular localization of TAPL. In transfected human ovarian carcinoma cells, TAPL has been localized in lysosomes (5). In contrast, green fluorescent protein-tagged TAPL was found in the endoplasmic reticulum of transfected COS-1 cells (4).

TAPL comprises an N-terminal transmembrane domain and a C-terminal nucleotide-binding domain, which contains all conserved motifs for ATP binding and hydrolysis (Walker A, Walker B, C-loop, Q-loop, and H-loop). Based on predictions of the membrane topology and sequence alignments, the transmembrane domain encompasses 10 transmembrane helices. To function as a transporter, TAPL must form a dimer with a counterpart. A protein-fragment complementation assay indicates that TAPL interacts with itself and not with TAP (8). These data have been challenged by very recent studies using green fluorescent protein- and DsRed-tagged TAPL and TAP1/2, suggesting that TAPL may form also heterodimers with TAP1 or TAP2 (9).

In this study, key issues regarding the TAPL function were addressed. We could demonstrate that TAPL forms a homodimeric complex, functioning as a specific and ATP-dependent peptide transporter. The transport characteristics and substrate specificity are determined, using a large selection of peptides and combinatorial peptide libraries.

EXPERIMENTAL PROCEDURES

Materials—8-Azido-[α-³²P]ATP was purchased from ICN. Peptides and peptide libraries were synthesized by Fmoc (*N*-(9-fluorenyl)methoxycarbonyl) solid phase chemistry (10). For immune detection of TAPL, rabbit antiserum was raised against the C terminus of TAPL (DFTAGHNEPVANGSHKA) and affinity-purified. The His-tag and Strep-tag of TAPL were detected by a monoclonal anti-His antibody (Novagen) and streptactin-horseradish peroxidase conjugate (IBA, Göttingen, Germany), respectively. Protein determination was performed by the Bradford method (Pierce).

Cloning and Expression of TAPL—Human TAPL (AF216494) with either a C-terminal His$_{10}$-tag (TAPL-H) or a Strep-tag II (TAPL-S) were cloned by PCR into pFastBac1 (Invitrogen) using the following sense and antisense primers: hTAPL-H-BamHI, CGATTAGGATCCATGCG-

---

[1] The abbreviations used are: ABC, ATP-binding cassette; MHC, major histocompatibility complex; TAP, transporter associated with antigen processing; TAPL, TAP-like; TAPL-H, His$_{10}$-tagged TAPL; TAPL-S, Strep-tagged II TAPL; Ni-NTA, nickel nitrilotriacetic acid; AMP-PNP, adenosine 5′-(β,γ-imino)triphosphate; ATPγS, adenosine 5′-*O*-(thiotriphosphate).

GCTGTGGAGG; hTAPL-H-SalI, CCTATAGTCGACTCAGTGATGGT-
GATGGTGATGGTGATGGTGGTGCTGGCCTTGTGACTGCC; hTAPL-
S-XhoI, CGATTACTCGAGATGCGGCTGTGGAAGG; hTAPL-S-SphI,
CCTATAGCATGCTCATTTTTCGAACTGCGGGTGGCTCCAAGCGCT-
GGCCTTGGACTGCC. Baculovirus generation, virus infection, and
protein expression were performed as described (11).

Pull-down Assays—Membranes (0.5 mg of total protein) prepared as
described (12) were washed with pull-down buffer (phosphate-buffered
saline, 15% glycerol) and resuspended in 100 μl of pull-down buffer
containing 2% digitonin and 1% (v/v) protease inhibitor mix (50 mg/ml
4-(2-aminoethyl)benzenesulfonyl fluoride hydrochloride, 0.1 mg/ml
aprotinin, 1 mg/ml leupeptin, 0.5 mg/ml pepstatin A, and 15.6
mg/ml benzamidine). After a 30-min incubation on ice, samples were
centrifuged for 30 min at $100,000 \times g$. Solubilized proteins were incu-
bated with Ni-NTA magnetobeads (Sigma) for 60 min on ice. After three
washing steps with pull-down buffer containing 0.2% digitonin, the
co-precipitated proteins were analyzed by SDS-PAGE (10%) and
Western blotting.

Peptide Binding and Transport Assays—Peptide binding and trans-
port were performed with either ^{125}I-labeled (11) or fluorescein-labeled
peptides (13). Peptide binding was carried out as described (14). For
transport, membranes (25 μg of protein) were preincubated with 3 mM
ATP and 5 mM $MgCl_2$ in 50 μl of phosphate-buffered saline for 1 min at
32 °C. The transport reaction was started by adding peptides and
stopped by the addition of 200 μl of ice-cold phosphate-buffered saline,
10 mM EDTA after 2 min at 32 °C, if not mentioned otherwise. Subse-
quently, samples were transferred to microfilter plates preincubated
with 0.3% polyethylene imine (MultiScreen plates, Durapore mem-
brane, 0.65-μm pore size, Millipore). Filters were washed twice with
250 μl ice-cold phosphate-buffered saline, 10 mM EDTA. The amount of
radiolabeled peptide was quantified by γ-counting. If fluorescein-la-
beled peptides were used, the filters were incubated with 250 μl of
elution buffer (phosphate-buffered saline, 1% SDS) for 5 min. The
fluorescent peptides were quantified by a fluorescence plate reader
($\lambda_{ex/em}$ 485/520 nm; BMG, Polarstar Galaxy). Background transport
activity was measured in the presence of apyrase (1 unit) and in the
absence of ATP. The data of the ATP-dependent and peptide-dependent
transport were fitted by the Michaelis-Menten equation. To determine
the IC_{50} value for half-maximal inhibition by vanadate the following
equation was used,

$$v = \frac{v_{max}}{1 + \left(\frac{[\text{vanadate}]}{IC_{50}}\right)^{\text{slope}}} + bg \qquad (\text{Eq.1})$$

where v, v_{max}, and bg represent the transport rate, maximal transport
rate, and background, respectively.

8-Azido-[α-^{32}P]ATP Photocross-linking—Photocross-linking was per-
formed as described (11). After solubilization, the photocross-linked
TAPL was purified by streptactin-Sepharose and analyzed by SDS-
PAGE (10%), followed by transfer onto nitrocellulose membranes. Pho-
tocross-linked proteins were quantified by phosphorimaging (Phosphor-
Imager 445Si, Molecular Dynamics). The intensities (I) were plotted
against the 8-azido-ATP concentration and fitted with a Langmuir
isotherm (1:1). To determine the IC_{50} value for ATP, Equation 1 was
used. Applying the Cheng-Prusoff equation (15), the dissociation con-
stant K_i for ATP was derived from the IC_{50} value for ATP and the K_d
value for 8-azido-ATP,

$$K_i = \frac{IC_{50}}{1 + \frac{[\text{azido} - \text{ATP}]}{K_d}} \qquad (\text{Eq.2})$$

as shown in Equation 2.

<div align="center">RESULTS</div>

Expression and Homodimer Formation of TAPL—To analyze
the function of TAPL, the ABC half-size transporter was ex-
pressed in insect cells using recombinant baculoviruses. 48 h
after infection, cells were harvested, and TAPL was detected in
the membrane fraction using an antibody raised against the C
terminus of TAPL (Fig. 1A). Degradation products are not
detected, indicating that TAPL is a stable protein. Membranes
from insect cells infected with baculovirus coding for tapasin
(16) show no cross-reaction. TAPL has an apparent molecular
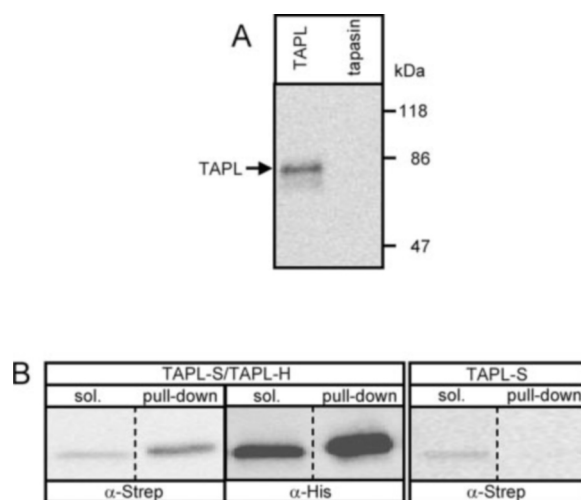mass of 70 kDa, which is identical to ABCB9 expressed in

FIG. 1. **Expression and homodimer formation of TAPL.** *A*, ex-
pression of TAPL. Membranes (0.5 μg of protein/lane) from insect cells
infected with baculovirus-TAPL-S or baculovirus-tapasin (16) were an-
alyzed by Western blot with TAPL-specific antibodies. *B*, homodimer
formation of TAPL. Membranes (0.5 mg of protein) containing His$_{10}$-
tagged TAPL (*TAPL-H*) and Strep-tagged TAPL (*TAPL-S*) or only
TAPL-S were solubilized by digitonin. TAPL was precipitated with
Ni-NTA magnetobeads and analyzed by specific detection of the His$_{10}$-
tag or Strep-tag. Corresponding soluble (*sol.*) and pull-down fractions
were loaded on the same gel. The exposure time of the Western blot was
identical.

human cells (5). The difference from the theoretical value
(M_{th} = 84 kDa) can be explained by the aberrant behavior of
highly hydrophobic proteins on SDS-PAGE. An analogous shift
has been observed for TAP1 (17).

To provide direct evidence about the oligomeric state of
TAPL, we co-expressed TAPL with a C-terminal His-tag
(TAPL-H) and Strep-tag (TAPL-S). After solubilization with
digitonin, TAPL-H was precipitated via its His-tag by Ni-NTA
beads. Bound proteins were analyzed by SDS-PAGE and West-
ern blotting. As shown in Fig. 1B, TAPL-S was co-precipitated
with TAPL-H, demonstrating that TAPL interacts with itself.
TAPL-S expressed alone does not bind to the Ni-NTA beads.
Similarly, after precipitation of TAPL-S by streptactin beads,
we could detect TAPL-H with His-tag-specific antibodies (data
not shown). In summary, TAPL interacts with itself, forming a
homodimeric complex.

ATP-dependent Peptide Transport by TAPL—We next fo-
cused on the function of the homodimeric complex. Interest-
ingly, TAPL and TAP share a sequence identity of ≥49% with
respect to the putative peptide-binding region. Therefore, we
examined whether homodimeric TAPL can bind peptides in the
same manner as the heterodimeric TAP complex (18, 19).
TAPL-containing membranes were incubated with radiola-
beled peptide RRYQKSTEL. Bound peptides were quantified
by rapid filter assays. However, no peptide-binding activity
was detected up to a peptide concentration of 1 μM.

To analyze the transport function of TAPL, TAPL-containing
membranes were incubated in presence of radiolabeled peptide
(RRYQKSTEL, 1 μM) and ATP (3 mM) for 2 min at 32 °C.
Strikingly, TAPL-containing membranes show an ATP-
dependent peptide transport, which is 30-fold above the back-
ground in absence of ATP (Fig. 2A). In contrast, tapasin-con-
taining membranes are deficient in peptide transport. Of note,
the fluorescein-labeled peptide (RRYQNSTC(Φ)L, Φ symbol-
izes the fluorophore) is transported as efficiently as the radio-
labeled peptide, thus showing that the transport activity is not
biased by the labeling technique and that TAPL has some steric
flexibility with regard to its substrates, transporting peptides
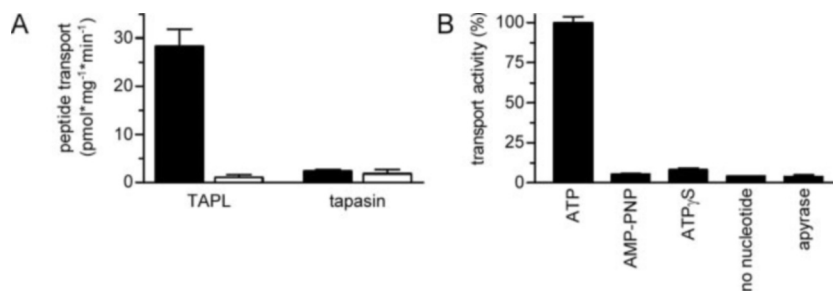even with bulky fluorophores (Fig. 2B). The transport strictly

FIG. 2. **Specific and ATP-dependent peptide transport by TAPL.** Membranes (25 μg of protein) prepared from insect cells were incubated with 1 μM ^{125}I-labeled RRYQKSTEL (*A*) or 1 μM fluorescein-labeled RRYQNSTC(Φ)L (*B*). Transport assays were performed in presence or absence of 3 mM nucleotide for 2 min at 32 °C. *A*, TAPL-specific peptide transport. Transport activity of TAPL- and tapasin-containing membranes were determined in the presence (*filled bars*) and absence of ATP (*open bars*). *B*, ATP-dependent peptide transport. Peptide transport was measured in presence of 3 mM nucleotides. The data resemble the mean of three measurements, and the *error bars* give the S.D.

requires ATP hydrolysis, because non-hydrolyzable ATP analogues, such as AMP-PNP and ATPγS, do not energize peptide translocation by TAPL.

Transport Characteristics and Specific Inhibition of TAPL—We next undertook a detailed analysis of the transport parameters of TAPL. At 1 μM fluorescent peptide RRYNSTC(Φ)L, the transport is linear up to 3 min corresponding to an initial translocation rate of 97 pmol of peptides/mg of protein/min (Fig. 3*A*). After 4 min, the transport reached equilibrium. Depletion of peptide can be excluded, as only 20% of the added peptides are transported. Taking a phospholipid-to-protein mass ratio of 1:1, a vesicle diameter of 250 nm, and the area of a phospholipid molecule of 0.60 nm^2, peptides are accumulated 60-fold in the lumen. This value is an underestimation, because membrane vesicles might not all contain TAPL. These data demonstrate that TAPL pumps peptides against a gradient. Correspondingly, all transport assays were performed for 2 min to ensure that initial rates are measured.

As a fingerprint of the transporter, we determined the Michaelis-Menten kinetics of TAPL with respect to peptide and ATP concentrations. As shown in Fig. 3*B*, the transport follows Michaelis-Menten kinetics with a $K_{m(\text{pep})}$ of 6.8 $\pm$ 2.8 μM for the peptide RRYQNSTC(Φ)L. Even at the highest peptide concentration, the uptake is linear within the first 3 min, hence confirming that initial transport rates are measured (Fig. 3*B*, *inset*). The maximal transport activity (v_{max}) is 181 $\pm$ 7 pmol mg^{-1} min^{-1}. Based on quantitative immunoblotting using purified protein as reference, the turnover number of TAPL was estimated to ~30 peptides/min.

We then examined the peptide transport in dependence on the ATP concentration. Again, the transport follows Michaelis-Menten kinetics with a $K_{m(\text{ATP})}$ of 17.6 $\pm$ 2.4 μM for ATP (Fig. 3*C*). Finally, the inhibition of the ATP-driven transport by orthovanadate was studied (Fig. 3*D*). In some ABC transporters, vanadate can trap MgADP after ATP hydrolysis in the nucleotide-binding site, thereby acting as a specific inhibitor. In the case of TAPL, peptide transport is fully blocked at 100 μM vanadate, and half-maximal inhibition occurs at a vanadate concentration of 11.5 $\pm$ 1.0 μM, which is similar to other ABC transporters (20, 21).

Finally, the temperature and pH optimum for TAPL was investigated (Fig. 3, *E* and *F*). The temperature and the pH-dependent transport show a bell-shaped curve with an optimum at 37 °C and pH 7.0.

Nucleotide Specificity of TAPL—To study the binding and specificity of nucleotides for TAPL, we performed 8-azido-ATP photocross-linking studies. 8-Azido-ATP is a competitive substrate for ATP with a similar specificity constant (k_{cat}/K_m) as ATP (data not shown). As shown in Fig. 4*A*, photolabeling of TAPL is ATP-specific and saturable. Assuming a Langmuir-type (1:1)-binding curve, the apparent affinity constant for

8-azido-ATP was determined as 4.5 $\pm$ 0.9 μM. Equal amounts of purified TAPL in each lane are confirmed by immunodetection (data not shown). It should be noted that only apparent binding constants for 8-azido-ATP are derived depending on a variety of parameters. However, in each case the apparent binding constants are below the "real" values. As the affinity of 8-azido-ATP is often higher than that of ATP, the binding constant of ATP was determined in competition experiments. In the presence of 2.5 μM 8-azido-[α-32P]ATP, an IC$_{50}$ value of 140 $\pm$ 18 μM was obtained for ATP (Fig. 4*B*). Based on the apparent affinity of 8-azido-ATP, an apparent dissociation constant for MgATP of 90 $\pm$ 12 μM was derived.

ABC transporters can be energized by different nucleoside triphosphates. We therefore investigated the nucleotide specificity of TAPL by competition experiments using 8-azido-[α-32P]ATP photocross-linking (Fig. 4*C*). GTP, AMP-PNP, ADP (70% inhibition), and UTP (30% inhibition) showed slightly reduced affinity for TAPL compared with ATP, whereas CTP and AMP did not block 8-azido-ATP binding. Thus, the nucleotides analyzed can be ranked in three categories: ATP as the substrate with the highest affinity for TAPL; GTP, AMP-PNP, ADP, and UTP with an intermediate affinity; and CTP as well as AMP with a very low affinity. This nucleotide-binding preference is reflected in the transport activity, where GTP shows 40%, UTP 20%, and CTP 10% of the ATP-driven transport activity (Fig. 4*D*). These data prove that TAPL has some predilection for purine bases similar to other ABC transporters (17, 22).

Peptide Specificity of TAPL—We first focused on the length of peptides recognized and translocated by TAPL. To circumvent any effect of the peptide sequence, we applied combinatorial peptide libraries $(X)_n$ from 4 to 59 residues in length, where X represents all 19 amino acids, excluding cysteine, in equimolar distribution. The libraries were radiolabeled and initial ATP-dependent transport rates were followed within the first 3 min. Strikingly, TAPL manifested a strong preference for peptides with six residues and longer (Fig. 5*A*). Shorter peptides are not transported. The transport optimum is reached with peptide libraries of ~23 residues. TAPL appears to be highly promiscuous, because 10-fold longer peptides show the same transport efficiency than the X_6 peptide library.

This remarkably broad specificity leads to the question of how peptides of such broad length distribution are recognized by TAPL. Free N and C termini are required for peptide recognition of MHC class I molecules and the TAP complex (reviewed by Refs. 23 and 24). To address the role of the N and C terminus in peptide recognition by TAPL, we applied radiolabeled 8-mer peptide libraries (X_8) with modified termini. As displayed in Fig. 5*B*, peptide transport is blocked either by modification of the N terminus (acetylation) or C terminus (amidation), suggesting that the α-amino group and the C-terminal carboxyl group are
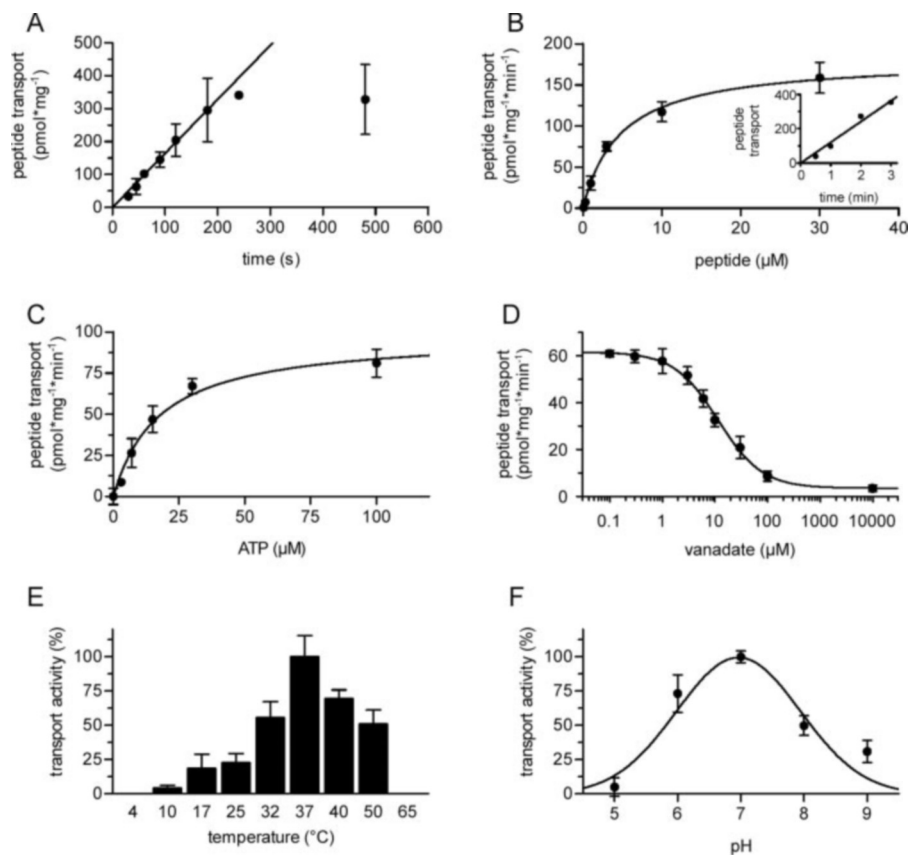
FIG. 3. **Kinetic parameters of peptide transporter TAPL.** TAPL-containing membranes (25 μg protein) were incubated with fluorescein-labeled peptide (RRYQNSTC(Φ)L, 1 μM) for 2 min at 32 °C in presence of 3 mM ATP, if not stated differently. Transported peptides were quantified by fluorescence detection. *A*, time dependence of the transport activity. The data for the first 3 min of transport were fitted by a linear regression. After 4 min a maximum of 340 pmol of peptide/mg of protein was reached. *B*, peptide dependence of the transport activity. The data were fitted by the Michaelis-Menten equation with a $K_{m(\text{pep})}$ value of 6.8 $\pm$ 2.8 μM. The maximal transport activity (v_{max}) is 181 $\pm$ 7 pmol mg^{-1} min^{-1}. The linear peptide uptake within the first 3 min at highest peptide concentration (30 μM) is illustrated in the *inset*. *C*, ATP dependence of the transport activity. Peptide transport was followed under saturating peptide concentration (20 μM). The data were fitted by the Michaelis-Menten equation with a $K_{m(\text{ATP})}$ value of 17.6 $\pm$ 2.4 μM. *D*, inhibition of peptide transport by vanadate. Peptide transport was performed in presence of 20 μM peptide. The data were fitted by Equation 1 yielding an IC$_{50}$ value of 11.5 $\pm$ 1.0 μM. *E*, temperature dependence of the transport activity. Peptide transport was carried out at temperatures between 4 and 65 °C. *F*, pH dependence of transport activity. Peptide transport was followed between pH 5 and 9 using citrate buffer (pH 5), phosphate buffer (pH 6 and 7), Tris buffer (pH 8), and tricine buffer (pH 9). The data represent the mean of three independent measurements, and the *error bars* give the S.D.

both essential for peptide recognition.

At last, we investigated the stereoselectivity of TAPL. For this purpose, the transport of a 9-mer peptide (RRYNASTEL) was compared with its D-isomer (inverse peptide, rrynastel) and a D-isomer with inverted sequence (retroinverse peptide, letsanyrr). In contrast to the L-isomer, the D-isomer and the retroinverse peptide are not transported by TAPL. In the retroinverse peptide, the side chains have the same orientation as in the L-peptide, but the peptide backbone is inverted. These results indicate that peptides are recognized via the peptide backbone including the free N and C terminus as well as via side chain interactions. In summary, TAPL is a stereospecific peptide transporter with broad length and sequence preference.

DISCUSSION

Human ABC transporters of the subfamily B are multifaceted in their physiological function, cellular location, interaction partners, and substrates, which range from hydrophobic drugs to bile salts and peptides. The transport function of most members of this subfamily has not yet been determined. In this study, we could elucidate the functional unit, the transport activity, and substrate specificity of the half-size transporter ABCB9 (TAPL). TAPL interacts with itself, forming a homodimeric complex. This functional unit is essential and sufficient for specific peptide transport, which strictly requires

ATP-hydrolysis. TAPL translocates peptides with a minimum of 6 residues via recognition of the peptide backbone, including free N and C termini.

TAPL cannot restore antigen presentation via MHC class I molecules in TAP1- or TAP2-deficient cells.[2] Noticeably, if peptides with an *N*-glycosylation targeting sequence are applied, only a minor fraction of peptides transported by TAPL become *N*-glycosylated, thus indicating that TAPL translocates peptides into a post-endoplasmic reticulum compartment, where they can accumulate. In contrast to TAPL, the TAP complex transfers peptides into the endoplasmic reticulum-lumen, where they can only be trapped by *N*-glycosylation (25). We therefore conclude that TAPL is not involved in the classic route of antigen processing via MHC class I molecules.

Homodimeric TAPL and heterodimeric TAP do not only share high sequence identity but also the function as peptide transporter. Moreover, the recognition principle of both ABC transporters seems to be similar. Both transport complexes can only translocate peptides with free N and C termini (10). Moreover, the stereospecificity for peptides with L-amino acids is conserved. D-Peptides or retroinverse D-peptides are not transported by TAPL. Taken together these results indicate that the
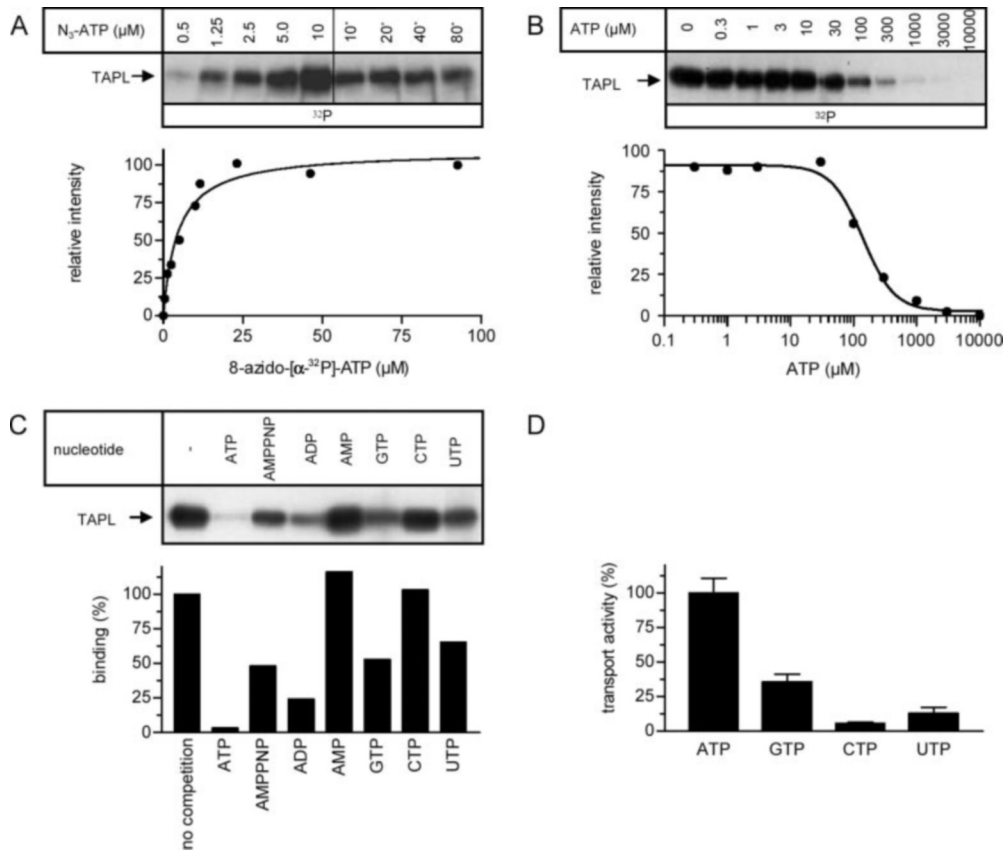

FIG. 4. **Nucleotide specificity of TAPL.** TAPL-containing membranes (100 μg of protein) were incubated with 8-azido-[α-^{32}P]ATP for 10 min at 4 °C and treated as mentioned under "Methods and Materials." *A*, 8-azido-[α-^{32}P]ATP photocross-linking. For concentrations of 10 μM and above (indicated by *stars*), 8-azido-[α-^{32}P]ATP was supplemented with non-radioactive 8-azido-ATP (1:5). The intensities of substituted 8-azido-[α-^{32}P]ATP were adjusted to the non-substituted 8-azido-[α-^{32}P]ATP by comparing the intensities at 10 μM. The intensities quantified by phosphorimaging were plotted against 8-azido-ATP concentration and fitted with a Langmuir isotherm (1:1) resulting in an apparent dissociation constant (K_d) of 4.5 $\pm$ 0.9 μM. *B*, ATP competition of 8-azido-ATP photocross-linking. TAPL-containing membranes were incubated with 2.5 μM 8-azido-[α-^{32}P]ATP and different ATP concentrations. The intensities were plotted against the ATP concentration and fitted to Equation 1 leading to an IC$_{50}$ value of 140 $\pm$ 18 μM. *C*, nucleotide-binding specificity of TAPL. TAPL-containing membranes were incubated in the presence of 5 μM 8-azido-[α-^{32}P]ATP with 1 mM nucleotide each. *D*, nucleotide-specific peptide transport. Peptide transport was performed with 30 μM nucleotide in presence of 1 μM fluorescein-labeled RRYQNSTC(Φ)L for 2 min at 32 °C. The data resemble the mean of three independent measurements, and the *error bars* give the S.D.
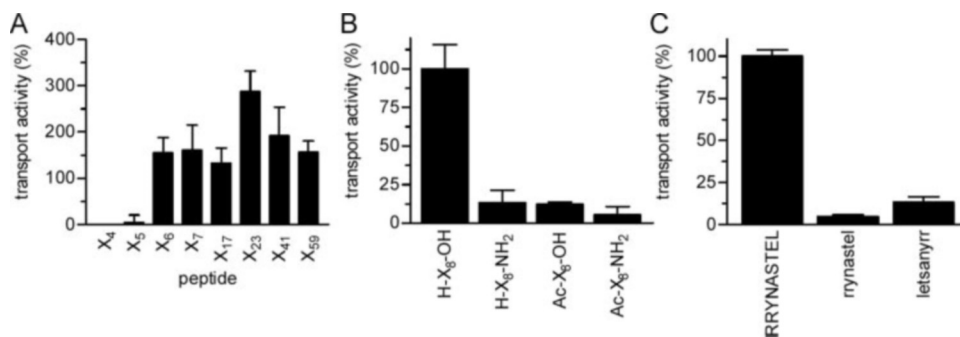

FIG. 5. **Peptide specificity of TAPL.** *A*, length specificity of TAPL. The transport activity of TAPL-containing membranes (25 μg of protein) for radiolabeled peptide libraries (1 μM) were measured in presence of 3 mM ATP. The data were collected at 1, 2, and 3 min at 32 °C and approximated by linear regression. The transport rates were related to the transport of the peptide RRYQKSTEL. *B*, peptide transport of peptides with modified N and C termini was analyzed at 3 mM ATP for 2 min at 32 °C. *C*, stereoselectivity of TAPL. Peptide transport of RRYNASTEL, of its D-isomer rrynastel, and of the retroinverse D-peptide letsanyrr was conducted in presence of 3 mM ATP for 2 min at 32 °C. The data represent the mean of three independent measurements, and the *error bars* indicate the S.D.

orientation of the side chains as well as the peptide backbone is essential for peptide recognition. Strikingly, both peptide transporters differ in their length specificity. Whereas TAP most efficiently transports peptides from 8 to 12 amino acids in length optimized for peptide loading of MHC class I molecules (26), TAPL has a much broader length specificity with an optimum for peptides of ~23 amino acids. These data suggest that TAPL is not involved in peptide loading of MHC I mole-

cules. Whether splice variants of TAPL possess different peptide specificities and whether they also vary in localization and transport efficiency still has to be addressed in future studies.

The TAPL and TAP complexes show strong differences in peptide binding. TAP binds peptides with high affinity, ~100–300 nM (13, 18, 19). In contrast, we could not detect any peptide binding to TAPL using rapid filter binding or equilibrium binding assays. This observation correlates with a high $K_{m(pep)}$

value for peptide transport (6.8 μM). Therefore, TAPL seems to function as a vacuum cleaner (low affinity, high capacity), removing peptides from the cytosol. Similar differences between homologous transporters were also found for the renal and intestinal peptide transporters, PEPT1 and PEPT2, which transport di- and tripeptides in a proton-dependent manner (27, 28). Interestingly, PEPT2 resembles the high affinity and low capacity transporter, whereas PEPT1 translocates peptides with high capacity but binds the substrates with low affinity. Reasons for the different peptide affinities of TAP and TAPL must reside in the structure of the peptide-binding site.

TAPL exploits the chemical energy of ATP to drive peptide transport. Interestingly, the Michaelis-Menten constant $K_{m(\text{ATP})}$ for TAPL (17.6 μM) is 4–20-fold lower than for P-glycoprotein, cystic fibrosis transmembrane conductance regulator, TAP, and maltose permease from *Escherichia coli* (11, 21, 29, 30). Based on the physiological ATP concentration, this $K_{m(\text{ATP})}$ value ensures that TAPL is always fully active if peptides are present. The apparent affinity constant of ATP for TAPL (90 μM) is in the same range as that of other ABC transporters (31–33). Interestingly, the apparent affinity constant of TAPL for ATP, which is smaller than the "real" binding constant, is higher than the $K_{m(\text{ATP})}$ value, indicating that the ATP-binding step is followed by intermediates before final hydrolysis occurs (34). With respect to the complex cross-talk and communication among the peptide-binding site, nucleotide-binding domains, and the translocation pore (35), a multistep process can be easily imagined.

In this study, we could decipher the functional unit, transport activity, and substrate specificity of TAPL, which are important steps toward the understanding of the physiological function of the transport complex. It is tempting to speculate that TAPL is involved in the transport of peptides, generated by proteasomal degradation of endogenous proteins in the cytosol, into the MHC class II compartment for cross-presentation in dendritic cells. This hypothesis is supported by the finding that MHC class II molecules are loaded with peptides from endogenous proteins in a TAP-independent manner (36). However, this speculation contrasts with the expression of TAPL in Sertoli cells (5), which do not contain MHC class II molecules. Future studies will elucidate these pending issues.

REFERENCES

1. Davidson, A. L., and Chen, J. (2004) *Annu. Rev. Biochem.* **73,** 241–268
2. Schmitt, L., and Tampé, R. (2002) *Curr. Opin. Struct. Biol.* **12,** 754–760
3. Dean, M., Rzhetsky, A., and Allikmets, R. (2001) *Genome Res.* **11,** 1156–1166
4. Yamaguchi, Y., Kasano, M., Terada, T., Sato, R., and Maeda, M. (1999) *FEBS Lett.* **457,** 231–236
5. Zhang, F., Zhang, W., Liu, L., Fisher, C. L., Hui, D., Childs, S., Dorovini-Zis, K., and Ling, V. (2000) *J. Biol. Chem.* **275,** 23287–23294
6. Kobayashi, A., Hori, S., Suita, N., and Maeda, M. (2003) *Biochem. Biophys. Res. Commun.* **309,** 815–822
7. Yan, G., Shi, L., and Faustman, D. (1999) *J. Immunol.* **162,** 852–859
8. Leveson-Gower, D. B., Michnick, S. W., and Ling, V. (2004) *Biochemistry* **43,** 14257–14264
9. Kobayashi, A., Maeda, T., and Maeda, M. (2004) *Biol. Pharm. Bull.* **27,** 1916–1922
10. Uebel, S., Kraas, W., Kienle, S., Wiesmüller, K. H., Jung, G., and Tampé, R. (1997) *Proc. Natl. Acad. Sci. U. S. A.* **94,** 8976–8981
11. Chen, M., Abele, R., and Tampé, R. (2003) *J. Biol. Chem.* **278,** 29686–29692
12. Heintke, S., Chen, M., Ritz, U., Lankat-Buttgereit, B., Koch, J., Abele, R., Seliger, B., and Tampé, R. (2003) *FEBS Lett.* **533,** 42–46
13. Neumann, L., and Tampé, R. (1999) *J. Mol. Biol.* **294,** 1203–1213
14. Chen, M., Abele, R., and Tampe, R. (2004) *J. Biol. Chem.* **279,** 46073–46081
15. Cheng, Y., and Prusoff, W. H. (1973) *Biochem. Pharmacol.* **22,** 3099–3108
16. Koch, J., Guntrum, R., Heintke, S., Kyritsis, C., and Tampé, R. (2004) *J. Biol. Chem.* **279,** 10142–10147
17. Meyer, T. H., van Endert, P. M., Uebel, S., Ehring, B., and Tampé, R. (1994) *FEBS Lett.* **351,** 443–447
18. van Endert, P. M., Tampé, R., Meyer, T. H., Tisch, R., Bach, J. F., and McDevitt, H. O. (1994) *Immunity* **1,** 491–500
19. Uebel, S., Meyer, T. H., Kraas, W., Kienle, S., Jung, G., Wiesmüller, K. H., and Tampé, R. (1995) *J. Biol. Chem.* **270,** 18512–18516
20. Ambudkar, S. V., Lelong, I. H., Zhang, J., Cardarelli, C. O., Gottesman, M. M., and Pastan, I. (1992) *Proc. Natl. Acad. Sci. U. S. A.* **89,** 8472–8476
21. Landmesser, H., Stein, A., Bluschke, B., Brinkmann, M., Hunke, S., and Schneider, E. (2002) *Biochim. Biophys. Acta* **1565,** 64–72
22. al-Shawi, M. K., and Senior, A. E. (1993) *J. Biol. Chem.* **268,** 4197–4206
23. Madden, D. R. (1995) *Annu. Rev. Immunol.* **13,** 587–622
24. Uebel, S., and Tampé, R. (1999) *Curr. Opin. Immunol.* **11,** 203–208
25. Neefjes, J. J., Momburg, F., and Hämmerling, G. J. (1993) *Science* **261,** 769–771
26. Koopmann, J. O., Post, M., Neefjes, J. J., Hämmerling, G. J., and Momburg, F. (1996) *Eur. J. Immunol.* **26,** 1720–1728
27. Daniel, H., Morse, E. L., and Adibi, S. A. (1991) *J. Biol. Chem.* **266,** 19917–19924
28. Leibach, F. H., and Ganapathy, V. (1996) *Annu. Rev. Nutr.* **16,** 99–119
29. Li, C., Ramjeesingh, M., Wang, W., Garami, E., Hewryk, M., Lee, D., Rommens, J. M., Galley, K., and Bear, C. E. (1996) *J. Biol. Chem.* **271,** 28463–28468
30. Sarkadi, B., Price, E. M., Boucher, R. C., Germann, U. A., and Scarborough, G. A. (1992) *J. Biol. Chem.* **267,** 4854–4858
31. Qu, Q., Russell, P. L., and Sharom, F. J. (2003) *Biochemistry* **42,** 1170–1177
32. Lapinski, P. E., Raghuraman, G., and Raghavan, M. (2003) *J. Biol. Chem.* **278,** 8229–8237
33. Horn, C., Bremer, E., and Schmitt, L. (2003) *J. Mol. Biol.* **334,** 403–419
34. Fersht, A. (1997) *Enzyme Structure and Mechanism*, W. H. Freeman and Company, New York
35. van der Does, C., and Tampé, R. (2004) *Biol. Chem.* **385,** 927–933
36. Dani, A., Chaudhry, A., Mukherjee, P., Rajagopal, D., Bhatia, S., George, A., Bal, V., Rath, S., and Mayor, S. (2004) *J. Cell Sci.* **117,** 4219–4230